FINITE ELEMENT ANALYSIS OF VEHICLE INTERIOR NOISE IN A SERIES OF STRUCTURAL MODELS OF INCREASED COMPLEXITY

VB Georgiev Department of Aeronautical and Automotive Engineering, Loughborough University,
VV Krylov Loughborough, Leicestershire LE11 3TU, UK

1 INTRODUCTION

Numerical methods of structural-acoustic analysis of vehicle bodies are widely used by new car developers to predict and reduce structure-borne vehicle-interior noise. Modern finite element (FE) techniques can represent real vehicle structures in great detail, which leads to the numerical results comparable with the experimental ones [1,2]. However, in many cases the numerical analysis of complex vehicle structures does not allow to explain certain physical characteristics typical for the model. In this regard, investigation of simplified structural models by FE methods could provide some additional useful and practically important information. Futhermore, the use of simplified models for numerical investigations can give the opportunity for a quick change of the model parameters and immediate estimation of the results of alteration. As a result, simplified models can assist in better understanding of vehicle structural-acoustic behaviour and in identifying the most important parameters influencing structure-borne noise generation in vehicle compartments.

Vibrations of the simplest type of structures that can be used to emulate real vehicle structures, flexible rectangular boxes, have been investigated analytically using some simple approximations [3,4]. On the other hand, using further simplifications of the models, e.g. considering a rectangular box structure with one vibrating wall only [5,6,7], one can obtain exact analytical solutions that can provide an even deeper insight into the physical mechanisms of structural-acoustic interaction. Recently, a new simplified model of vehicle body structure, QUASICAR, built up of a non-circular cylindrical shell has been investigated both theoretically and experimentally [8,9,10]. The main advantage of this structure was the possibility of obtaining the approximate analytical solution for sound pressure in the vehicle interior as a function of the model parameters, road irregularity, vehicle speed, properties of vehicle suspensions, etc.

Some authors utilised simplified box models to verify different optimisation procedures for noise reduction [11-13]. In this regard, simplified models assisted in a quicker estimation of the proposed design modifications from the point of view of noise reduction.

In spite of some important advances achieved using the above-mentioned simplest structural models, there is still a wide gap between such models and highly detailed ones analysed by car manufacturers by means of specially developed commercial software based mainly on finite and boundary element techniques. The simple box-based models, although very imprecise, are more or less well understood, whereas the latter ones, having rather complex geometrical forms and material properties, are very difficult to interpret and, as a result, very difficult to modify in a desirable way of reduction of generated structure-borne noise.

In the light of the above, the main aim of this paper is to investigate a series of simplified vehicle structural models with different degrees of complexity in order to bridge the currently existing gap between the simplest rectangular box models and much more detailed models of real vehicles. The sequence of models to be investigated consists of six simplified structures of increased complexity. The simplest of them represents the above-mentioned rectangular box structure and the most complex one gives an unambiguous impression of an average car compartment. The main objective

of the study was to investigate the influence of gradual changes in structural modifications on structure-borne vehicle interior noise.

2 DESCRIPTION OF THE SIMPLIFIED VEHICLE MODELS

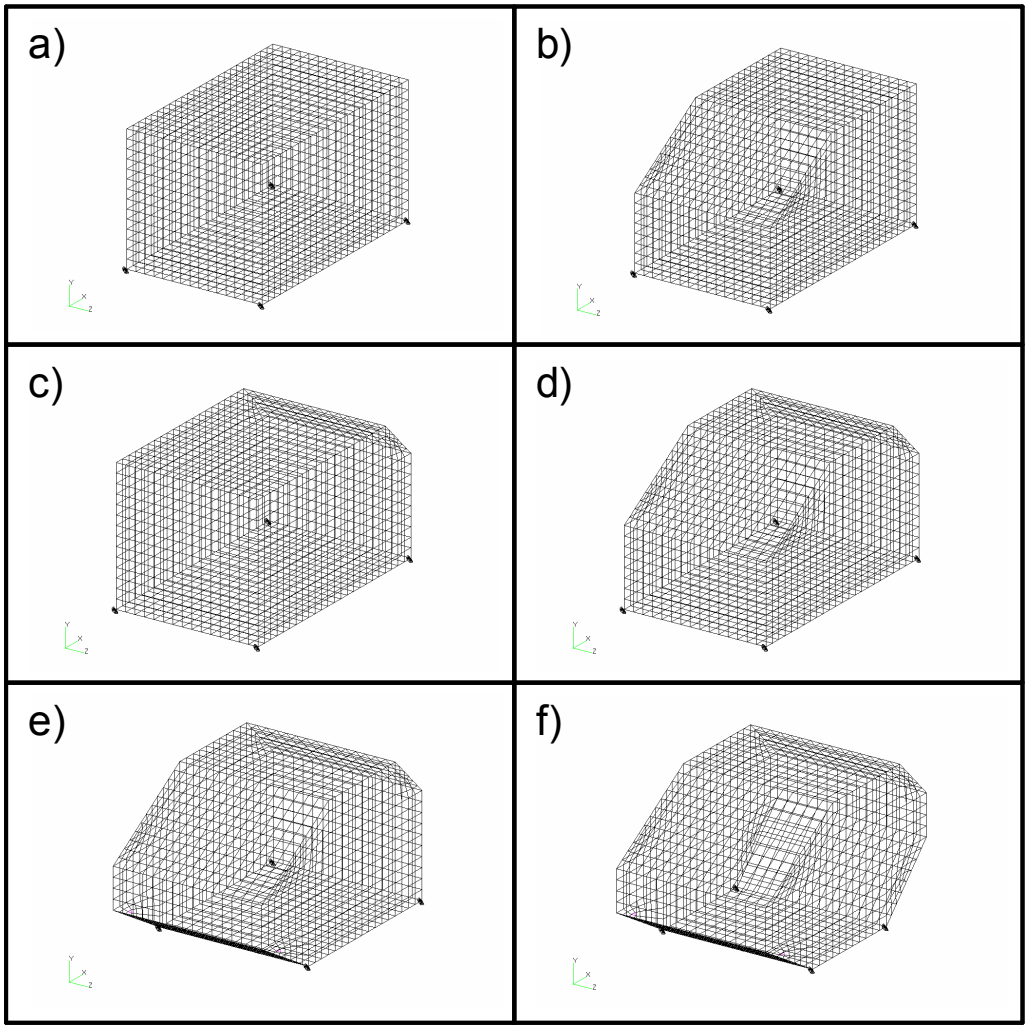

Figure 1. Geometry of the models: a) model “A” b) model “B” c) model “C” d) model “D” e) model “E” and f) model “F”

As was mentioned above, a sequence of the six simplified vehicle models of increased complexity was investigated. For the sake of simplicity, these models are identified as model “A”, “B”, …, and “F” (see Fig. 1). The models have characteristic dimensions of a typical medium size car: 2.4, 1.4, and 1.5 m respectively in X, Y, and Z directions. The thickness of all walls is 8 mm, which corresponds to a fundamental structural frequency matching the fundamental frequency of a typical car body, in the range of 5-20 Hz. The number of structural and acoustic finite elements and element nodes is nearly the same for all models. The relevant information can be found in Table 1. For the structural part of analysis, “CQUAD” finite elements were used, whereas for the acoustic part, “CHEXA” finite elements were employed. The mesh size was consistent with the maximum frequency range of interest, which was 500 Hz (a wavelength of 0.6626 m). The recommended minimum number of finite elements per wavelength is six. This means that the finite element size must be less than 0.11 m. In the light of this, the size of 0.1 m has been chosen. Simply supported

boundary conditions were imposed at the bottom corners of the models, as it can be seen in Fig. 1. Note that structural modifications associated with the more complex models represent main design elements, such as windscreens, rear windows, etc. In spite of the structural changes from one model to another, the input and output points, corresponding to the positions of a disturbing force and a receiver respectively, remained the same to provide a meaningful comparison of the results obtained for different models.

Model	Number of structural FE	Number of structural nodes	Number of acoustic FE	Number of acoustic nodes
A	1812	2013	5040	6000
B	1744	2022	4980	5305
C	1780	2050	5025	6283
D	1712	2068	5872	6603
E	1664	2063	5808	6810
F	1595	2533	5712	6940

Table 1. Numbers of structural and acoustic finite elements and nodes for each model

3 UNCOUPLED STRUCTURAL AND ACOUSTIC MODES

Starting from the geometrically simplest model, model “A”, representing a flexible rectangular box, the structural and acoustic normal modes and natural frequencies of all uncoupled models under consideration have been calculated and analysed.

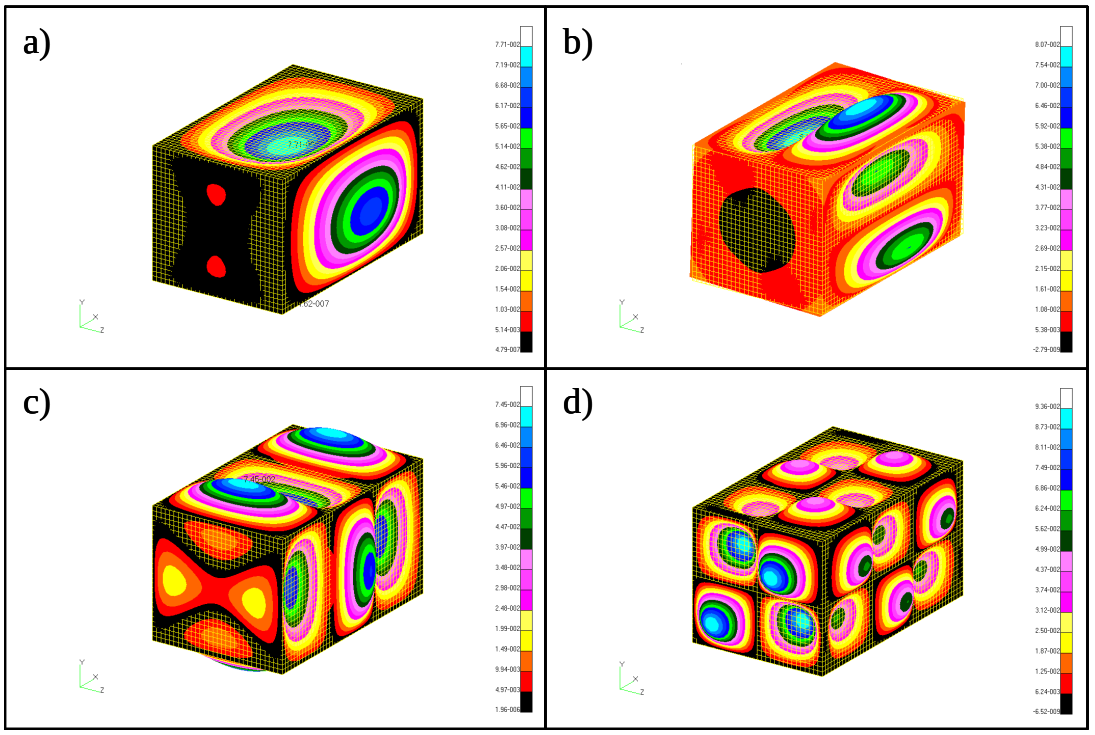

Figure 2. Some structural modes of model “A”

Figure 2 shows some structural modes of the uncoupled model “A”. The results show in particular that there are no symmetric and anti-symmetric structural modes in a flexible rectangular box. To explain these results, some additional calculations have been conducted to elucidate the influence of geometrical symmetry on the existence of symmetric and anti-symmetric modes. As a result, model “A” could be qualitatively interpreted as a structure consisting of three coupled resonators for elastic waves that are formed by three closed-loop waveguides supporting the predominant normal modes of vibration. However, the discussion of these aspects is beyond the scope of the present paper, and the detailed account of this study will be published elsewhere.

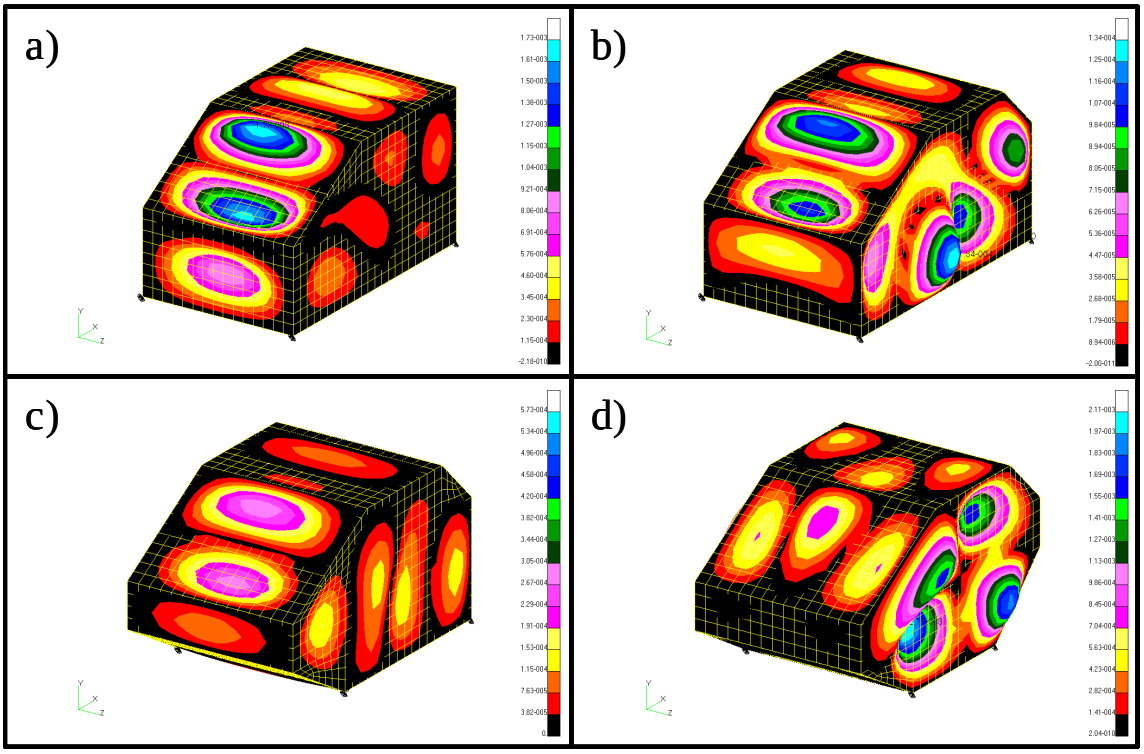

Figure 3. Some structural modes of: a) model “B” at 81.251Hz b) model “D” at 74.081Hz c) model “E” at 76.778 Hz and d) model “F” at 78.371 Hz

In contrast to the initial model “A”, the other models are constructed of plates that are different not only in size but also in form. Some structural modes of the uncoupled models “B”, “D”, “E” and “F” are shown in Fig. 3. One can see that modal shapes of the whole structures are strongly influenced by the forms of the plate compounds. As expected, for rectangular compounds simulating windscreens and roofs, the modal shapes are simple and largely resemble the forms observed for a rectangular box (see Fig. 2), whereas for side plates, that have rather complex geometrical forms, the modal shapes are quite irregular.

Figure 4 and Table 2 represent some of the acoustic modes and natural frequencies of the above models. The comparison between analytically calculated natural frequencies and those calculated by using finite element software for model “A” shows a good agreement and validates the chosen mesh size. Moreover, in the medium frequency range, for mode (6, 2, 1), the exact solution defines the natural frequency of 489.44 Hz, whereas the finite element program gives 499.67 Hz. In other words a maximum relative error of 2 % at the highest frequency of interest has been achieved, which guarantees the correct and reliable numerical results for all other frequencies.

Analysing the data in Table 2, one can notice some interesting results. For example, the second natural frequency, 110.64 Hz - for the mode (0, 0, 1), stays constant for all models under

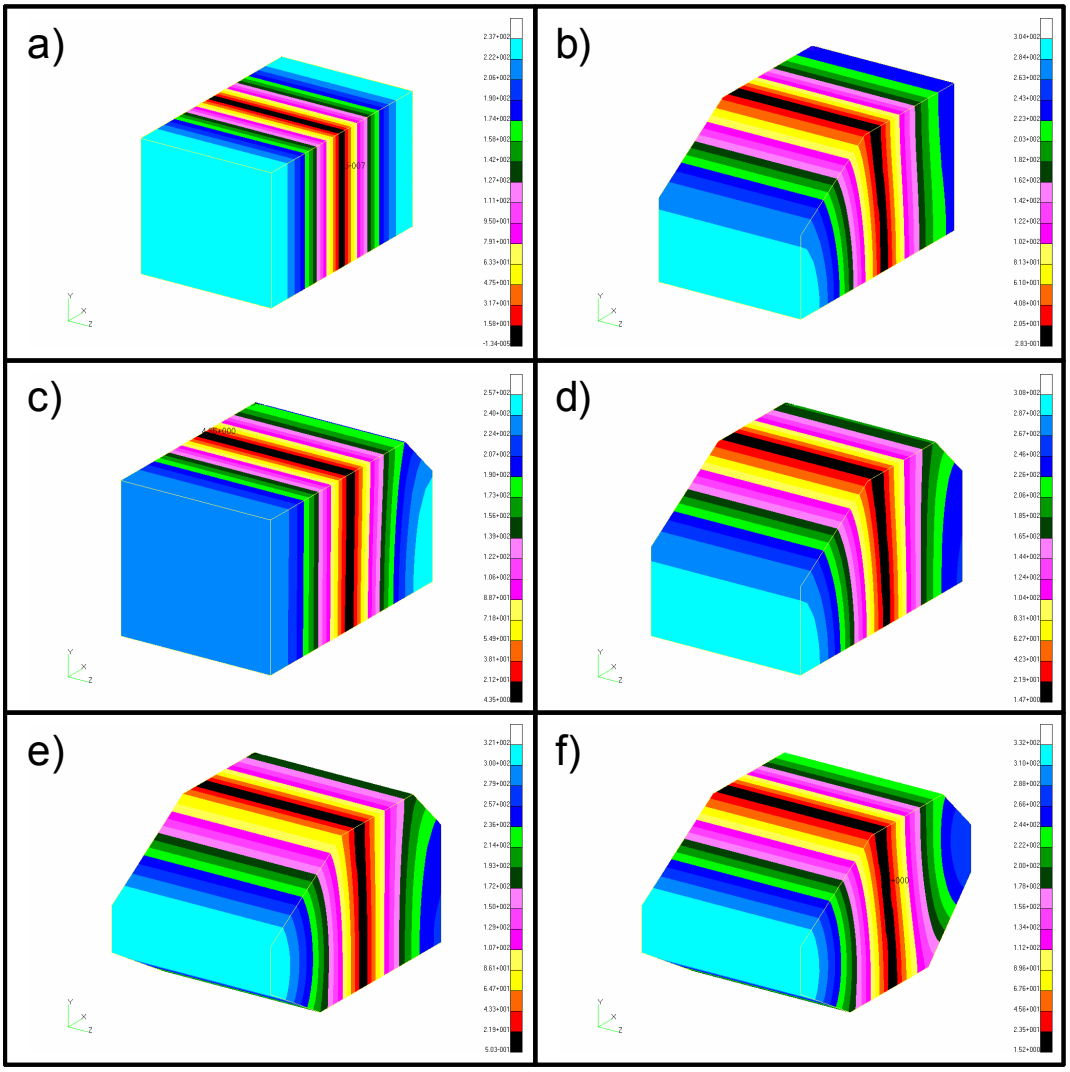

Figure 4. First acoustic mode in each model

consideration, regardless of the structural modifications. Although it was not recorded in Table 2, the next natural frequency in z-direction (mode (0, 0, 2)) also does not change and stays at 222.48 Hz for all models.

4 FREQUENCY RESPONSE ANALISIS OF COUPLED MODELS

The frequency response functions (FRF's) at specific structural and acoustic spatial points have been calculated for different models. For this purpose, four structural points, where an external disturbing force was applied to simulate the effects of vehicle suspensions, and two acoustic points - at a driver's and a passenger's ear, where the interior noise was measured, were of particular interest. Various combinations of input and output signals calculated for these points form the set of FRF's that was analysed. As was mentioned above, simply supported boundary conditions at the corner nodes in the bottom plate were imposed for simulating more realisticaly the vibrations of vehicle compartment. The amplitude of an external disturbing force was set as 200 N for all subsequent calculations.

?	Model A (exact)	Model A (num.)	Model B (num.)	Model C (num.)	Model D (num.)	Model E (num.)	Model F (num.)
1	69.02 (1, 0, 0)	69.07 (1, 0, 0)	72.29 (1, 0, 0)	70.50 (1, 0, 0)	73.77 (1, 0, 0)	77.94 (1, 0, 0)	81.63 (1, 0, 0)
2	110.40 (0, 0, 1)	110.64 (0, 0, 1)	110.64 (0, 0, 1)	110.64 (0, 0, 1)	110.64 (0, 0, 1)	110.64 (0, 0, 1)	110.64 (0, 0, 1)
3	118.33 (0, 1, 0)	118.52 (0, 1, 0)	122.04 (0, 1, 0)	120.05 (0, 1, 0)	122.84 (0, 1, 0)	125.15 (0, 1, 0)	132.31 (0, 1, 0)
4	130.21 (1, 0, 1)	130.40 (1, 0, 1)	132.16 (1, 0, 1)	131.19 (1, 0, 1)	132.98 (1, 0, 1)	135.30 (1, 0, 1)	137.49 (1, 0, 1)
5	137.02 (1, 1, 0)	137.27 (1, 1, 0)	135.80 (2, 0, 0)	137.44 (2, 0, 0)	143.11 (2, 0, 0)	146.00 (2, 0, 0)	146.09 (2, 0, 0)
6	138.07 (2, 0, 0)	138.49 (2, 0, 0)	162.42 (1, 1, 0)	145.73 (1, 1, 0)	165.31 (1, 1, 0)	167.04 (0, 1, 1)	172.47 (0, 1, 1)
7	161.94 (0, 1, 1)	162.21 (0, 1, 1)	164.72 (0, 1, 1)	163.25 (0, 1, 1)	165.32 (0, 1, 1)	168.00 (1, 1, 0)	183.26 (2, 0, 1)
8	175.95 (1, 1, 1)	176.23 (1, 1, 1)	175.16 (2, 0, 1)	176.44 (2, 0, 1)	180.89 (2, 0, 1)	183.18 (2, 0, 1)	183.89 (1, 1, 0)
9	176.81 (2, 0, 1)	177.20 (2, 0, 1)	196.42 (3, 0, 0)	182.97 (1, 1, 1)	198.91 (1, 1, 1)	201.16 (1, 1, 1)	209.33 (3, 0, 0)
10	181.84 (2, 1, 0)	182.24 (2, 1, 0)	196.52 (1, 1, 1)	188.17 (2, 1, 0)	202.53 (3, 0, 0)	209.75 (3, 0, 0)	214.61 (1, 1, 1)

Table 2. First ten acoustic natural frequencies for the considered models

A comparison between pressure FRF's of different models was carried out to estimate the influence of the respective structural modifications on generated structure-borne interior noise. In this case, the external force was applied to the left front position simulating road disturbance acting through the left front tire, whereas the output position of the receiver was set at the driver's ear position. Frequency response functions were calculated in the frequency range from 0 to 500 Hz. The energy loss factor of all structures was chosen as 3 %.

Influence of air damping on sound pressure levels was examined by carrying out calculations for the model "A". Four damping coeffcients have been used, between 0.1 and 1.5 %. The numerical simulations have shown that the damping coefficients do not influence much on the noise levels. Before reaching the first acoustic resonance, at about 69 Hz, the sound pressure level depends only on structural vibrations, and the four graphs coincide completely. Above the first acoustic peak, the sound pressure responses behave differently, depending on the damping coefficient. For further calculations, a 1 % damping factor was adopted, similarly to the examples described in Ref. 14.

Figure 5 shows the pressure frequency response functions calculated for model "A" at the driver's ear position, depending on left and right, front and rear positions of the driving force. The same functions were calculated at the passenger's ear position as well. Keeping in mind that the first uncoupled acoustic natural frequency of the model "A" is about 69 Hz, the graphs presented in Fig. 5 can be regarded as consisting of two parts: below 69 Hz, where pressure FRF's are formed by structural vibrations of the model, and above 69 Hz, where pressure FRF's are formed by complex interaction of the structural and fluid vibrations. Although in the lowest frequency range, below the first acoustic resonance, noise levels are relatively low; this is a hazardous region from the practical point of view. In real vehicles, the idle operational regime of the engine is associated with frequencies of generated vibrations that are within this frequency range, thus causing unpleasant booming noise inside a vehicle compartment.

In the second part of the graphs in Fig. 5, above 69 Hz, the pressure FRF's reach their maxima and then decrease with oscillations. The maxima of generated sound pressure occur at different

frequencies for each of the figures. The maximum peak of FRF's for a driver's ear position is about 25 dB and occurs at 175 Hz. Similar calculations show that for a passenger's ear position the maximum peak is above 30 dB and occurs at about 130 Hz. This means that the same excitation can effect in different way a potential driver or passenger. In the case considered, the position of a passenger's ear is much more prone to high disturbing noise than a driver's ear position.

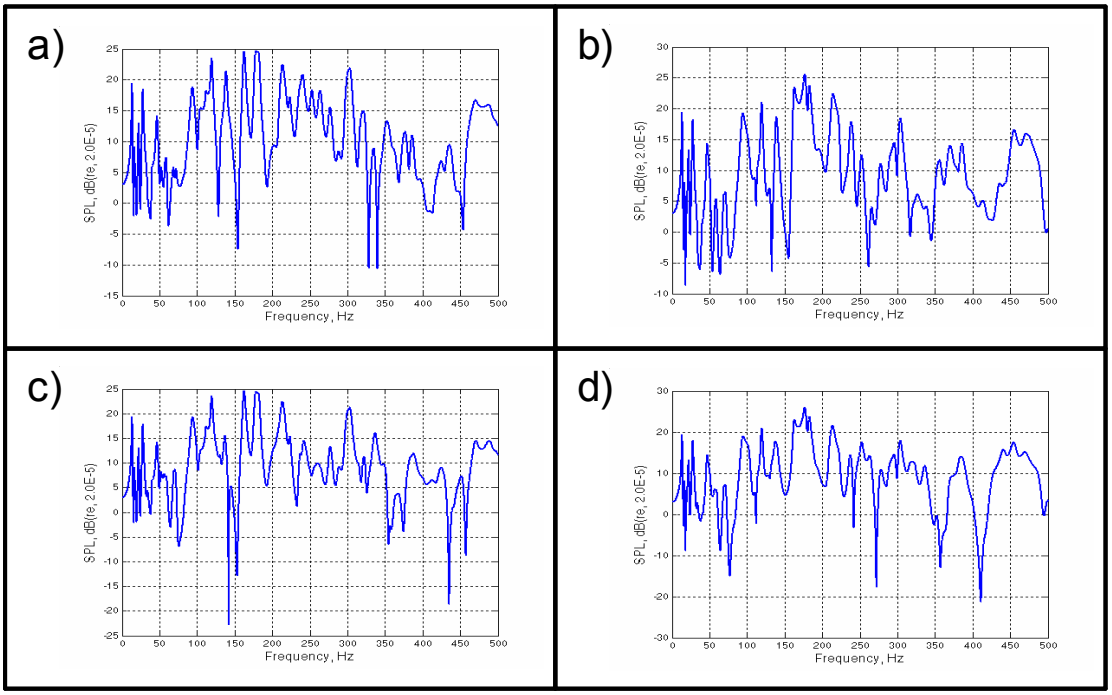

Figure 5. Pressure FRF's for model "A" in a driver's ear position due to a driving force applied at: a) left front b) right front c) left rear and d) right rear suspension

An important point is also the location of the disturbing force. If it acts close to a nodal line of a structural mode, then the force can not excite this structural mode and the resulting pressure response inside the car will be lower in amplitude. In principle, this can be used in practice for compensation of the external disturbance, when a designer considers the spattial pattern of structural vibrations and applies external disturbing forces to act at nodal lines. However, the complex geometry of the car structures and high density of the normal modes make the results arguable. In this regard, the comparison between FRF's due to different positions of the external force does not show significant difference for the overall pressure responses. This means that the disturbing forces applied to these positions excite more or less equal numbers of normal modes.

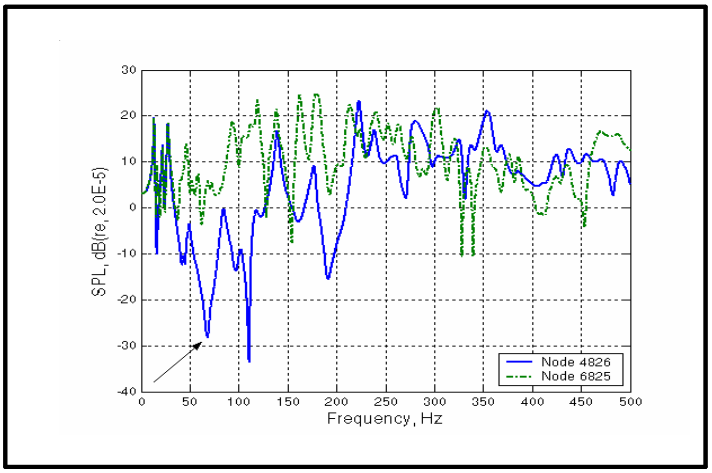

Figure 6. Sound pressure in driver's ear position (dash-dotted curve) and in a nodal point (solid curve)

The next key feature that can influence the pressure response in an enclosed cavity is the position of the receiver. Similarly to the location of the external force, the position of the receiver can increase or decrease the level of perceived noise. Assuming that the location of a receiver is close to a nodal line of a certain acoustic mode of the enclosure, the pressure response at that position will be lower in amplitude as compared to all other positions. In this regard, comparing the results for the maximum peak of pressure FRF's, as mentioned above, one can notice that sound pressure level in the passenger's ear position is by 5 dB higher than in the position of the driver's one.

Additional calculations have been carried out for better understanding of this important aspect. A position in the center of the model "A", which is nodal for the first four acoustic modes, was chosen and pressure FRF's were calculated. Figure 6 shows two FRF's in a driver's ear position, this is Node 6825 (dash-dotted curve), and at the nodal point, this is Node 4826 (solid curve). The decrease in sound pressure level for the latter graph is well noticeable in the frequency range from 50 to 200 Hz. For frequencies above 200 Hz, this location is not nodal any more and the sound pressure level becomes nearly the same as that for Node 4826. This simple example demonstrates that a preliminary acoustic analysis of a vehicle interior can provide sufficient information for establishing favourable positions at certain frequency range. It is also worth to know that, if a driver's or passenger's ear position is very close to the car walls, this may result in higher noise levels.

5 EFFECTS OF STRUCTURAL MODIFICATIONS

To estimate the influence of structural modifications in the models of increased complexity shown in Fig. 1 on generated structure-borne interior noise a comparison between pressure FRF's of every two adjacent models has been carried out. The receiver point was positioned at driver's ear, whereas the driving force was applied to a left front position in the bottom plate of the models for all simulations.

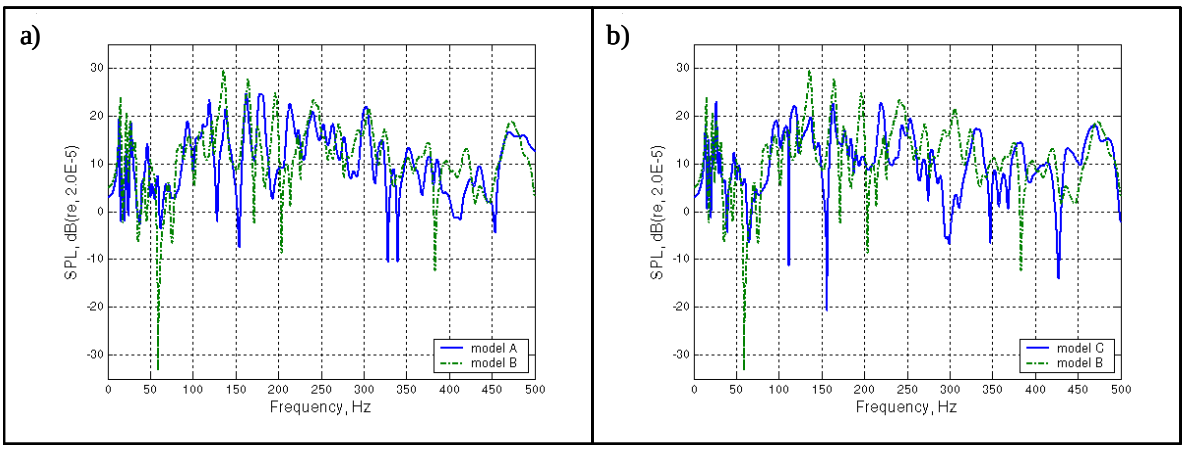

Figure 7. Comparison between sound pressure levels in a) model "A" (solid curve) and model "B" (dash-dotted curve) and in b) model"C" (solid curve) and model "B" (dash-dotted curve)

Figure 7 (a) shows the sound pressure levels in models "A" and "B" . At frequencies between 0 and around 70 Hz, both curves are nearly the same. At 70 Hz, there is a strong anti-resonance for model "B", which apparently can be explained by the fact that the driver's ear position for this model falls into a nodal line of the first acoustic mode. Above this frequency, the sound pressure level for the model "B" is slightly higher than for the model "A". Also, the resonant peaks are shifted due to the structural modification. From these results, one can conclude that the incline of the front surface raises the sound pressure level at driver's ear location as compared to the model "A", in which this front surface is vertical. This might be the result of the geometrical closeness between the receiver's position and the inclined front surface. Note that calculations of the structural normal modes for

these models show that small structural modifications that are not directly related to changes of mass density, stiffness and damping characteristics do not influence much the structural natural frequencies. Such modifications affect merely the spatial patterns of the acoustic normal modes, and this can be considered as a potential method of adjusting the receiver's position to a nodal line of the acoustic spatial pattern.

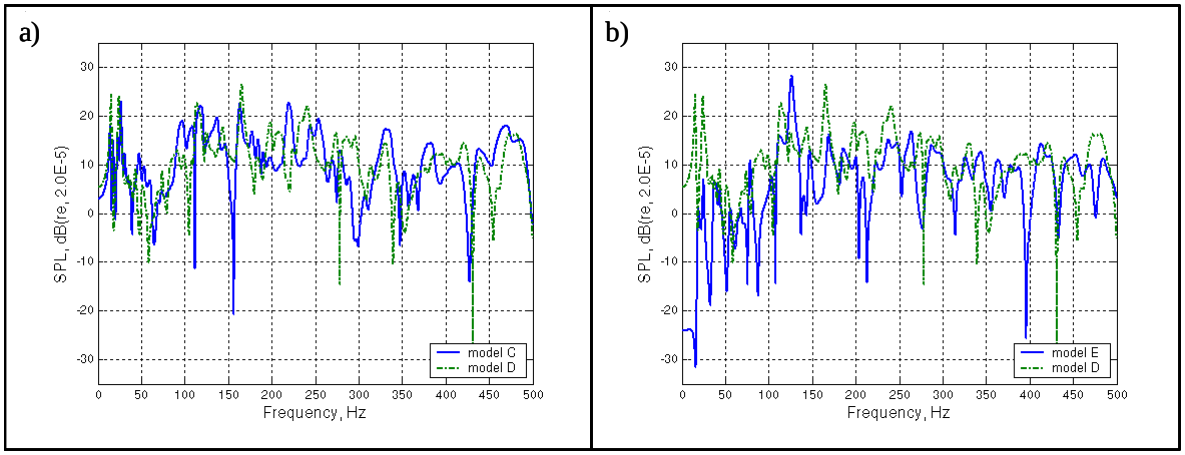

Figure 8. Comparison between sound pressure levels in a) model "C" (solid curve) and model "D" (dash-dotted curve) and b) model "E" (solid curve) and model "D" (dash-dotted curve)

Figures 7 (b) and 8 (a) demonstrate some noticeable changes in the pressure FRF's. In particular, it must be noted that sound pressure level in the model "C" is lower in comparison with the model "B" (Fig. 7 (b)). The reason for this might be the effect of the rear inclined surface in the model "C", which is smaller in size than the front inclined surface in the model "B".

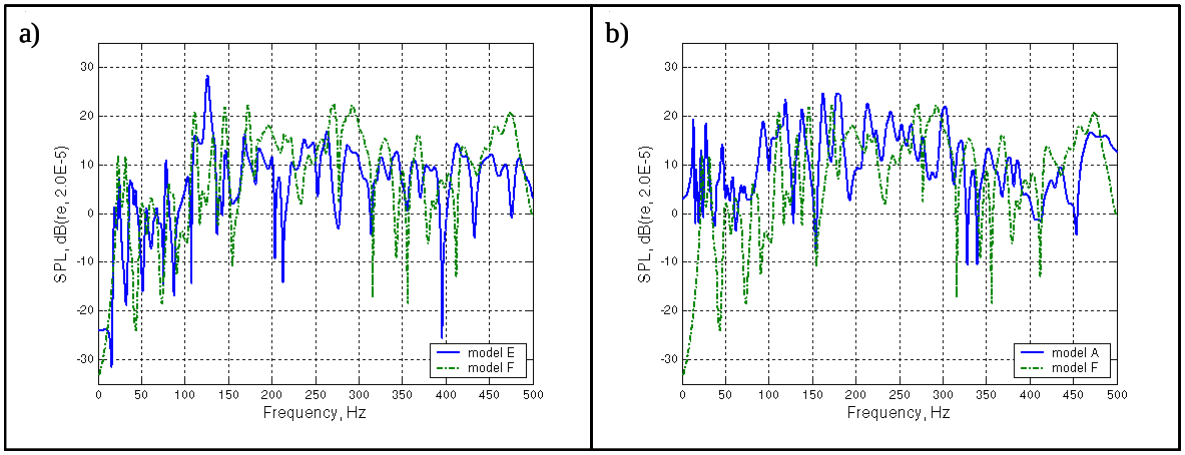

Figure 9. Comparison between sound pressure levels in a) model "E" (solid curve) and model "F" (dash-dotted curve) and b) model "A" (solid curve) and model "F" (dash-dotted curve)

Models "E" and "F" are slightly different from the rest of the models. Because of the required structural modifications, their bottom plates are shortened and the supports at the four corners are closer to the position of the disturbing force application. That might be the reason for the reduction of the sound pressure level below the first acoustic mode, at about 70 Hz, in models "E" and "F". This can be clearly seen in Figs. 8 (b) and 9 showing the comparison of the models "E" and "D", and models "E", "F" and "A" respectively. Note that, according to the curves in Figs. 7 – 9, the 'quietest' simplified model is model "E". The sound pressure FRF at driver's ear position calculated for this model is approximately by 4-5 dB lower compared to the others FRF's, except for the resonant peak

at about 125 Hz. On this stage, it is quite difficult to give a reasonable qualitative explanation of this interesting fact. Further numerical and analytical research would be required to achieve its better understanding.

6 CONCLUSIONS

In the present paper, a comprehensive numerical analysis of structural, acoustic and structural-acoustic properties of the series of six simplified vehicle models of gradually increased complexity has been carried out using MSC.Patran, MSC.Nastran. A number of frequency response functions (FRF's) have been calculated for different vehicle models. A comparison between pressure FRF's for every pair of adjacent models has been carried out to establish the impact of gradual structural modifications on structure-borne interior noise. It has been found that such modifications had little influence on the structural natural frequencies. However, they strongly affected the acoustic natural frequencies and normal modes as well as the resulting pressure FRF's. In the light of the above, some specific structural modifications could be used in practice for reducing structure-borne interior noise by adjusting the receiver's position into a nodal point of the appropriate acoustic modes.

7 REFERENCES

1. D.J. Nefske, J.A. Wolf, and L.J. Howell, Structural-acoustic finite element analysis of the automobile passenger compartment: A review of current practice. Journal of Sound and Vibration, 80 (1982), 247-266.
2. S.H. Sung and D.J. Nefske, A coupled structural-acoustic finite element model for vehicle interior noise analysis. J. Vibr., Acoust., Stress, Relaib. Design, Trans. of the ASME, 106 (1984), pp 314-318.
3. J. Liang and B.A.T. Petersson, Dominant dynamic characteristics of built-up structures. Journal of Sound and Vibration, 247(4) (2001), pp 703-718.
4. B.A.T. Petersson, Vibro-acoustic features of box-like structures. Proceedings of NOVEM 2005, Saint Raphael, France, April 2005 (on disk).
5. R.H. Lyon, Noise reduction of rectangular enclosures with one flexible wall. J. Acoust. Soc. Am. 35 (1963), pp 1791-1797.
6. A.J. Pretlove, Free vibrations of a rectangular panel backed by a closed rectangular cavity. Journal of Sound and Vibration, 2 (1965), pp 197-209.
7. A.J. Pretlove, Forced vibrations of a rectangular panel backed by a closed rectangular cavity. Journal of Sound and Vibration, 3 (1966), pp 252-261.
8. V.V. Krylov, Simplified analytical models for prediction of vehicle interior noise. Proceeding of the International Conference on Noise and Vibration Engineering, (ISMA 2002), Leuven, Belgium, Ed. P. Sas, vol. V (2002), pp. 1973-1980.
9. V.V. Krylov, S.J. Walsh, and R.E.T.B. Winward, Modelling of vehicle interior noise at reduced scale. Proceedings of Euronoise 2003, Naples, 2003 (on CD).
10. V.B. Georgiev, V.V. Krylov and R.E.T.B. Winward, Finite element calculations of structural-acoustic modes of vehicle interior for simplified models of motorcars. Proceedings of InterNoise *2004,* Prague, Czech Republic, pp 22-25, August 2004 (on disk).
11. S. Marburg, H.-J. Beer, J. Gier, H.-J. Hardtke, R. Rennert and F. Perret, Experimental verification of structural-acoustic modeling and design optimization. Journal of Sound and Vibration, 252(4) (2002), pp 591-615.
12. I. Hagiwara, D.W. Wang, Q.Z. Shi and R.S. Rao, Reduction of noise inside a cavity by piezoelectric actuators. Journal of Vibration and Acoustic, 125 (2003), pp 12-17.
13. J. Luo and H.C. Gea, Optimal stiffener design for interior sound reduction using a topology optimization based approach. Journal of Vibration and Acoustic, 125 (2003), pp 267-273.
14. NAS115-Fluid-Structure Analysis using MSC.Nastran Course Notes. MSC.Software, Los Angeles, 1996.